JOURNAL OF AIRCRAFT
Vol. 37, No. 4, July–August 2000

Navier–Stokes Computation of a Rapidly Deploying Spoiler

Seong-Wook Choi*
Korea Aerospace Research Institute, Taejon 305-333, Republic of Korea
and
Keun-Shik Chang†
Korea Advanced Institute of Science and Technology, Taejon 305-701, Republic of Korea

Transient aerodynamic response of an airfoil to a rapidly deploying spoiler is numerically investigated using a two-dimensional turbulent compressible Navier–Stokes flow model. The spoiler moving relative to a stationary airfoil is treated by an overset grid bounded by a dynamic domain-dividing line, the concept of which is developed first in this paper. The fluid-dynamic mechanism of the adverse lift because of the rapidly deploying spoiler is analyzed. Also the effect of spoiler deploying rate on the initial behavior of the aerodynamic response is expounded, which is of interest in view of active control technology and controller design for the spoiler. The results of present computation about the stationary as well as moving spoilers are relatively in good agreement with the existing experimental data.

Introduction

THE basic role of an aircraft control surface is to change the attitude of the aircraft to a desired state or, reversely, to restore the original attitude from the state disturbed by external forces such as a gust. Recently, much attention has been drawn to the active control technology (ACT), which can afford flight with relaxed stability and suppression of flutter, or reduction of vibration levels.[1] A spoiler deployed on the upper surface of a wing makes the flow separate, resulting in loss of lift and increase of drag. It is a device that is normally actuated in a very short time. These attributes lead to a variety of current and potential uses of the spoiler for the ACT of an aircraft.[2] The control system of an aircraft is required to respond rapidly with minimum overshoot or undershoot.[3] However, such unsteady nonlinear aerodynamic characteristics as adverse lift and time delay, associated with the rapid deployment of a spoiler, could create considerable difficulty in designing a proper feedback control system.[4] The adverse lift caused by the strong unsteady vortex behind the rapidly deploying spoiler is, on the other hand, considered favorable in order to generate higher dynamic lift.[5]

Most of the earlier experimental studies were conducted on the stationary and oscillating spoilers.[4–8] Only a few exceptional cases paid attention to the rapidly deploying spoiler. For example, Mabey[1] investigated the unsteady aerodynamic features of a rapidly deploying spoiler, recommending that time delay and adverse lift should be expressed as a function of nondimensional deploying time *Ut/c*. Consigny et al.[4] conducted experiments to examine the performance of a rapidly deploying spoiler on a supercritical airfoil. They concluded that significant amount of adverse lift and time delay could be resulted by the spoiler even at a moderate rate of rotation.

Numerical study on the spoiler aerodynamics was made by Tou and Hancock,[9] who used the panel method to investigate a stationary spoiler. Xu and Yeung[10] used the combined panel and discrete vortex method to model a moving spoiler, investigating reduction of adverse lift by the base venting, which had been observed earlier in their own experiment.[11] Although the panel and the discrete vortex methods are efficient, they require special models for the separated flows. Furthermore, accuracy could not be guaranteed by either of these methods for the high-Reynolds-number turbulent compressible flow.

Recently, Navier–Stokes equations have been used to study the stationary[12] and oscillating spoilers.[13] To compute the spoiler deployed rapidly to a large deflection angle, however, there are a few hindrances to overcome. One question is whether any of the existing turbulence models can appropriately simulate the dynamic turbulent flow behind a fully deployed spoiler. Another question is whether one can generate a moving grid system that covers the unsteady spoiler flapping from zero to a large deflection angle. In the present paper the Baldwin–Lomax turbulence model is used for the two-dimensional unsteady Navier–Stokes equations. To generate a dynamic Chimera grid system of the spoiler overlapping with the main airfoil grid, the concept of dynamic domain-dividing line (DDDL) is developed, which is defined as a line halving the distance between the airfoil and the spoiler at any instant. Following the experimental study of Yeung et al.,[11] we calculated the flow around a NACA 0012 airfoil with a 0.1c (10% chord length) spoiler. The adverse lift by the rapidly deploying spoiler has been clearly captured and validated by comparing with the experimental results. Aerodynamic characteristics such as time delay, undershoot, overshoot, and settling time of the airfoil response are analyzed as a function of spoiler deploying rate in this paper.

Numerical Methods

Two-dimensional unsteady compressible Navier–Stokes equations are written in an integral form on a moving grid system. For an arbitrary grid cell Ω with its boundary $\partial\Omega$, they are

$$\frac{\partial}{\partial t}\iint_{\Omega} \boldsymbol{Q}\,\mathrm{d}V + \int_{\partial\Omega} \boldsymbol{F}(\boldsymbol{Q})\cdot\hat{n}\,\mathrm{d}S = \int_{\partial\Omega} \boldsymbol{G}(\boldsymbol{Q})\cdot\hat{n}\,\mathrm{d}S \qquad (1)$$

where V is the cell volume, $\boldsymbol{Q}$ is the conservative variable vector, $\boldsymbol{F(Q)}$ is the inviscid flux vector, and $\boldsymbol{G(Q)}$ is the viscous flux vector.

In the time direction the second-order fully implicit scheme with a subiteration time-stepping procedure is used.[14] In a delta form, the equation becomes

$$\left[I\frac{V}{\Delta t} + \frac{\vartheta}{1+\varphi}\left(\frac{\partial \boldsymbol{R}}{\partial \boldsymbol{Q}}\right)\right](\boldsymbol{Q}^{p+1} - \boldsymbol{Q}^{p}) = -\frac{1}{1+\varphi}\boldsymbol{R}(\boldsymbol{Q}^{p}) - \frac{V}{\Delta t}\left(\boldsymbol{Q}^{p} - \frac{1+2\varphi}{1+\varphi}\boldsymbol{Q}^{n} + \frac{\varphi}{1+\varphi}\boldsymbol{Q}^{n-1}\right) \qquad (2)$$

where $\boldsymbol{R}(\boldsymbol{Q})$ is the residual vector brought about by summing the inviscid and viscous fluxes on the four faces of a cell. In Eq. (2) the $n-1$ and n level terms are taken from the solution of earlier time steps and, after iterating p times until convergence is made,

Received 14 September 1999; revision received 31 January 2000; accepted for publication 31 January 2000.

*Senior Researcher, Aerodynamics Department. Member AIAA.
†Professor, Department of Aerospace Engineering. Member AIAA.

the most recent value Q^{p+1} is assigned to the solution at time level $n+1$. The parameters ϑ and φ avail choice of different schemes: first- and second-order implicit schemes.

Equation (2) is solved using the point symmetric Gauss–Seidel (SGS) relaxation scheme in two steps, after Ok[15] :

Forward sweep:

$$C_1 \Delta Q^*_{i,j} = -R_{i,j} - C_2 \Delta Q^*_{i-1,j} - C_3 \Delta Q^*_{i,j-1} \tag{3}$$

Backward sweep:

$$C_1 \Delta Q_{i,j} = C_1 \Delta Q^*_{i,j} - C_4 \Delta Q_{i+1,j} - C_5 \Delta Q_{i,j+1} \tag{4}$$

where the coefficients $C_i (i = 1, 2, \ldots, 5)$ represent Jacobian matrices of the residual vector $R(Q)$ acquired from the cell under consideration and its four neighbor cells, namely,

$$C_1 = I \frac{V_{i,j}}{\Delta t} + \frac{\partial R_{i,j}}{\partial Q_{i,j}}, \qquad C_2 = \frac{\partial R_{i,j}}{\partial Q_{i-1,j}}, \qquad C_3 = \frac{\partial R_{i,j}}{\partial Q_{i,j-1}}$$

$$C_4 = \frac{\partial R_{i,j}}{\partial Q_{i+1,j}}, \qquad C_5 = \frac{\partial R_{i,j}}{\partial Q_{i,j+1}}$$

The inviscid flux terms are finite differenced with the Roe's flux-difference-splitting upwind method. Second-order spatial accuracy is obtained by the MUSCL approach with the flux limiter of Venkatakrishnan.[16] To treat the unsteady turbulent separated flow, the algebraic turbulence model by Baldwin–Lomax[17] is chosen in favor of computational robustness for the very complex flowfields as the present one.

Equation (2) can be applied to an overset grid system by simply inserting the hole-point flag i_b into the equations. During the point SGS relaxation procedure in Eqs. (3) and (4), data transfer for the variables ΔQ is achieved by the bilinear interpolation during each of the two sweeps. The new solution Q^{n+1} obtained on one grid system is also interpolated bilinearly for the solution on the other grid system. By this way, it was possible to elevate the Courant–Friedrichs–Lewy (CFL) number up to the level of a single grid.

Geometry and Grid

The configuration and dimension of the airfoil, NACA 0012, with a spoiler on its upper surface is given in Fig. 1. The 0.1 c spoiler is located at 0.7 c from the leading edge of the airfoil. A very small gap (0.0001 c) between the spoiler and the airfoil is maintained at the spoiler hinge in order to make the Chimera grid applicable. Figure 2 shows the initial clearance between the spoiler and the main airfoil at zero deflection angle: a vacuum state will be generated just after the sudden deployment of the spoiler without this clearance. For the reliable data communication of the Chimera grid, a larger initial clearance would be preferred. However, too large a gap will break smoothness of the airfoil surface to introduce undesirable airfoil characteristics.

The airfoil grid and the spoiler grid were generated independently and then overlaid in a time-dependent manner by the domain connectivity algorithm. The individual grid systems with smooth and noncrossing grid lines were generated layer by layer by the front-propagating scheme based on the elliptic equations.[18] The main

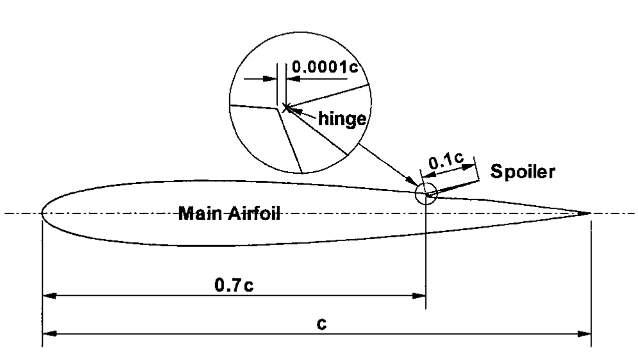

Fig. 1 Configuration of a NACA 0012 airfoil with a spoiler.

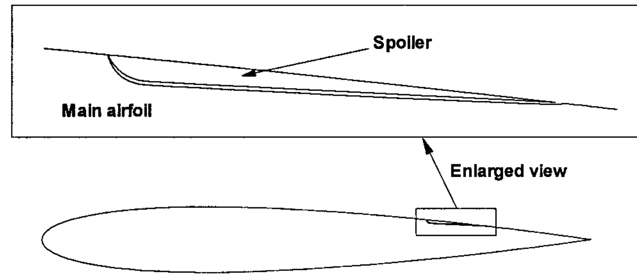

Fig. 2 Enlarged view around the spoiler.

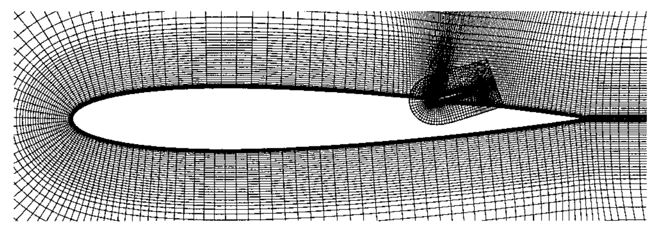

Fig. 3 Overset grid systems for an airfoil with a spoiler.

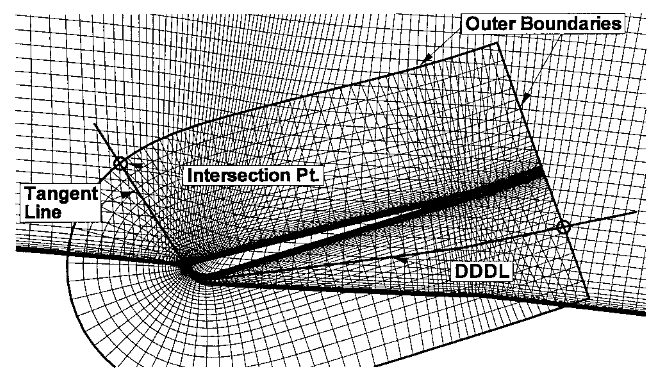

Fig. 4 Construction of the hole-cutting boundary using DDDL and tangent line.

airfoil grid and the spoiler grid had 301 ×65 and 101 ×41 C-type grid, respectively. The grid density of the airfoil grid system is made relatively higher behind the deployed spoiler where a large separated flow is expected (see Fig. 3). The minimum grid spacing at the wall is set to 0.00002c for the turbulent flow calculation.

To solve the flow equations on the Chimera grids, we need to search for the hole points to exclude them from computation and search for the fringe points to avail data communication. The present geometry, which has a very small gap at the spoiler hinge and in the initial clearance, makes it quite clumsy to apply the conventional Chimera grid because its hole-cutting boundary has to be defined on an outer layer some distance away from the body. To overcome this difficulty, we create a DDDL, which is made of a curve halving the distance between the airfoil and the spoiler plus a straight extension line tangentially connected to this curve (see Fig. 4). The tangent line is another straight line that is tangentially connected to the DDDL passing through the hinge gap. Joining the outer boundaries of the spoiler C-grid, the DDDL, and the tangent line at the intersection points, we have completely defined the hole-cutting boundary of the Chimera grid system. Figure 5 shows both the airfoil grid and the spoiler grid generated this way. With rotation of the spoiler, DDDL and the tangent line of the spoiler grid system are regenerated at each time step while the outer boundary is just under the solid body rotation.

Results and Discussion

Stationary Spoiler

A stationary spoiler is first calculated to check accuracy of the present Navier–Stokes code and applicability of the overset grid

Table 1 Spoiler deploying rate

Cases	Deploying rate, deg/s	Reduced rate, $\omega c/U$	Deploying time, ms	Reduced time, Ut/c
A	155	0.09	580	17.4
B	310	0.18	290	8.7
C	620	0.36	145	4.4
D	1240	0.72	72	2.2
E	2480	1.44	36	1.1
F	4960	2.88	18	0.5

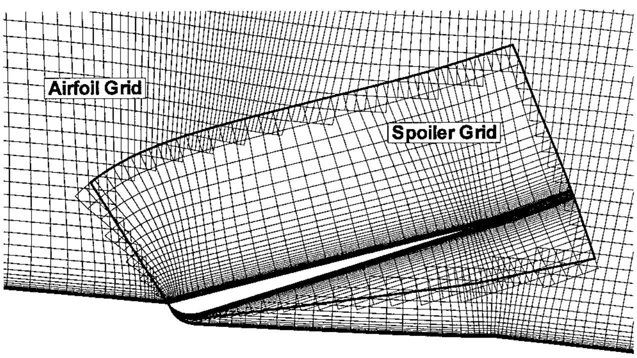

Fig. 5 Airfoil grid and spoiler grid at an instant; the hole cutting is shown here.

technique developed in this study. The main airfoil in this case is ONERA supercritical airfoil (RA16SC), which has experimental surface pressure data.[4] A 0.15c spoiler is hinged at 0.52c from the leading edge of the airfoil. There are some discrepancies in the spoiler configuration between the present and the experiment. The spoiler model used in the experiment has a thick and finite trailing edge, whereas it is modified in the present study to give a thin and sharp trailing edge. The overall shape and number of grid points used for the stationary spoiler are similar to the grid generated for the dynamic spoiler at an instant as in Fig. 3.

We consider two cases: a subsonic flow with the conditions $M_\infty = 0.3$, $Re = 1.9 \times 10^6$, $\alpha = 0$ deg, $\delta = 20$ deg, and a transonic flow with $M_\infty = 0.73$, $Re = 4.7 \times 10^6$, $\alpha = 0$ deg, and $\delta = 10$ deg. Time-accurate solution is required for the stationary spoiler because the vortex behind the deployed spoiler is not steady but shed periodically. We used the nondimensional time step $\Delta t = 0.01$ (CFL $\approx$ 1200) in the subsonic case and $\Delta t = 0.001$ (CFL $\approx$ 130) in the transonic case. To keep time accuracy, two subiterations were sufficient because more iterations did not bring in considerable difference: it is because we have already taken time steps small enough to achieve good resolution of the unsteady vortex.

Figures 6a and 6b represent the surface pressure coefficients averaged over a period for the subsonic and transonic flow cases, respectively. The subsonic flow at the spoiler deflection angle 20 deg shows good agreement with the experimental data from Ref. 4. Some discrepancy of the surface pressure is evident near the trailing edge partly because of the imperfect turbulence model and partly because of the shape modification of the spoiler trailing edge. A similar discrepancy was observed in the papers adopting Baldwin–Lomax turbulence model (see Refs. 12 and 13). For the transonic flow with the spoiler deflection angle 10 deg, the present results are generally in good agreement with the experiment except some differences on the lower surface where the shock is located and near the airfoil trailing edge. The pressure distribution around the spoiler hinge suggests that influence of the hinge gap is absolutely negligible.

Rapidly Deploying Spoiler

Using this computer code, investigation is now directed to the phenomenon of adverse lift and the effect of spoiler deploying rate on the unsteady airfoil characteristics. The freestream velocity is 12 m/s ($M_\infty = 0.035$), Reynolds number is 3.5×10^5 based on the airfoil chord length, and the deploying angle is 0 to 90 deg. Six different deploying rates shown in Table 1 are tested. Case C deploys

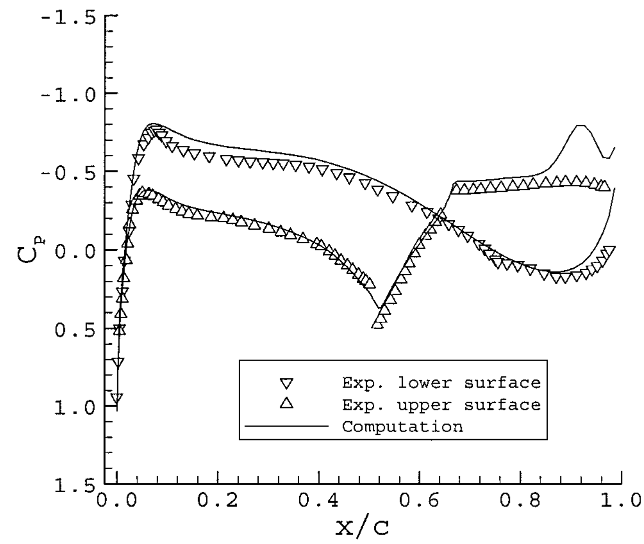

a) M_∞ = 0.3, α = 0 deg, Re = 1.9 $\times$ 10^6, and δ = 20 deg

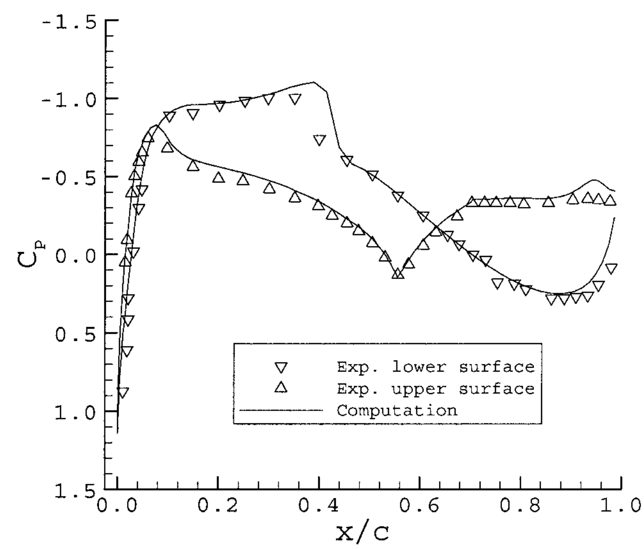

b) M_∞ = 0.73, α = 0 deg, Re = 4.7 $\times$ 10^6, and δ = 10 deg

Fig. 6 Time-averaged surface pressure coefficient of the RA16SC airfoil with a stationary spoiler.

the experimental conditions used in Ref. 11. The spoiler motion is represented by the ramp-like form[4,6] given by

$$\delta(t) = \delta_0 + \tfrac{1}{2}(\delta_1 - \delta_0)\{1 - \cos[\pi(t - t_0)/(t_1 - t_0)]\} \quad (5)$$

where $\delta_0 = 0$ deg, $\delta_1 = 90$ deg, $t_0 = 0$, and t_1 is the deploying time listed in Table 1. The time-dependent calculation is started with the steady-state flow at zero spoiler-deflection angle. We choose a time step equal to $\Delta t = 0.01$ (CFL $\approx$ 1000).

To analyze the aerodynamic response of the airfoil better, a few characteristic parameters are defined. Figure 7 shows a typical response caused by the rapid spoiler deployment, which resembles a system response by a unit step function in the control theory.[3] The initial decrease of lift C_{Lu} and the adverse lift C_{La} are defined respectively as the initial undershoot and overshoot of the lift coefficient. Their corresponding delay times are respectively, t_u and t_a, indicating how fast the aerodynamic forces respond to the spoiler movement. Settling time t_s is the time required until the initial steady lift coefficient C_{Li} is reduced to 90% of the final mean value C_{Lf}. It determines how fast the aerodynamic force converges to the oscillatory quasi-steady state.

In Fig. 8 the calculated lift, pitching moment, and drag coefficients are compared with the experimental data for the spoiler deploying rate 620 deg/s, case C. The initial steady lift is sustained until the

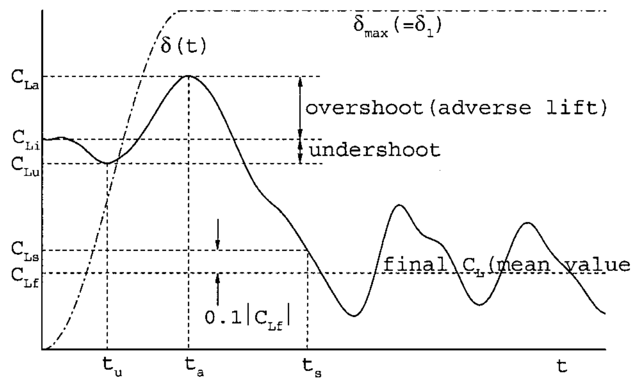

Fig. 7 Characteristic parameters of the aerodynamic response to a rapidly deploying spoiler.

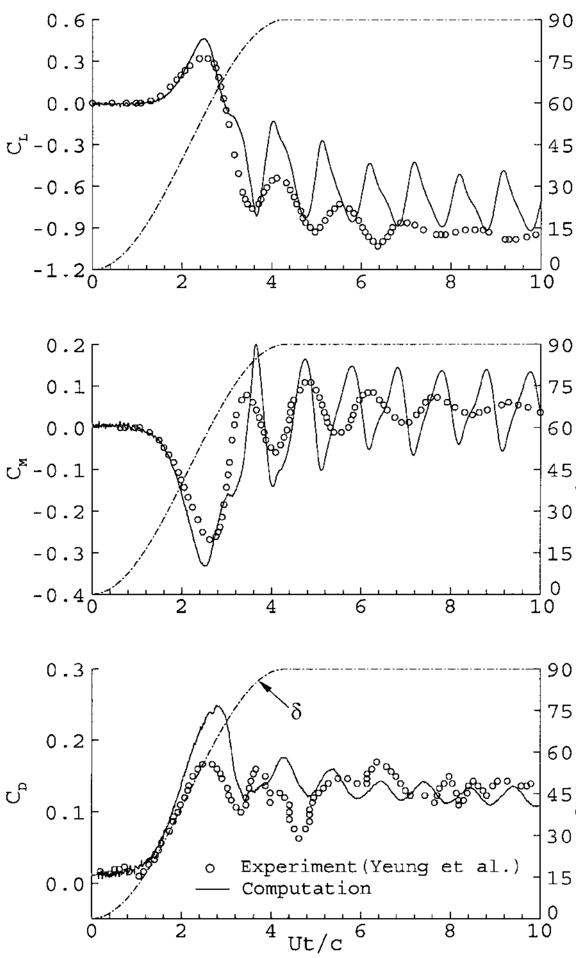

Fig. 8 Aerodynamic response to a rapidly deploying spoiler (ω = 620 deg/s).

spoiler is moved up to about 18 deg. The maximum adverse lift is visited when the deflection angle hits about 55 deg. Although its peak value is predicted somewhat higher in the present than in the experiment, the phase is accurately simulated. It definitely suggests that the time delay and the amplitude of the adverse lift can be reasonably predicted by the Navier–Stokes calculation. After full deployment of the spoiler, the oscillatory lift coefficient decays flat to the steady value in the experiment, whereas it is subject to quasi-steady oscillation having a characteristic amplitude and frequency in the present. Similar behavior has been reported in the previous investigations using a fully deployed stationary spoiler.[12,13] The validity of the present oscillatory final state may be less important be-

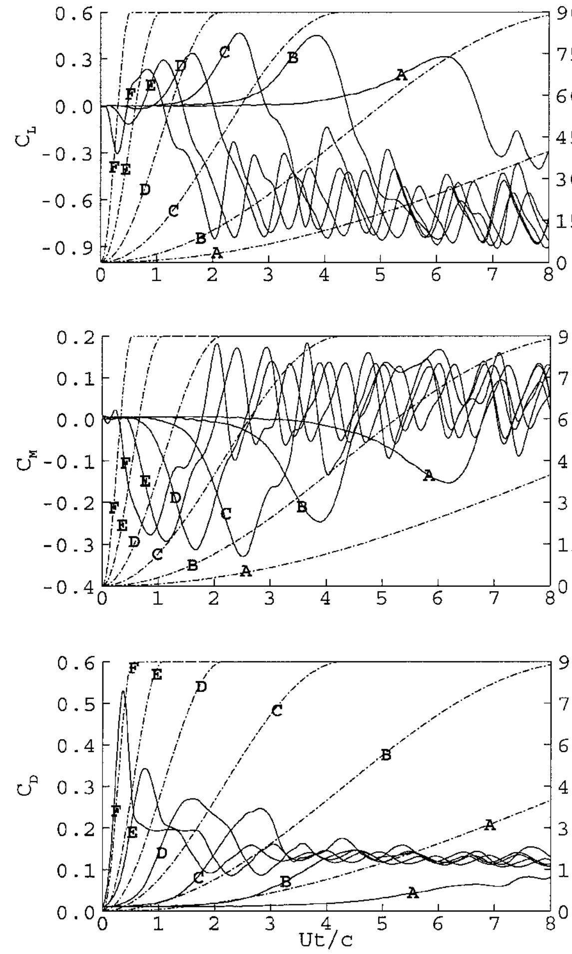

Fig. 9 Aerodynamic response with depending on the deploying rate.

cause the focus of the present study is on the transient aerodynamic behavior. Before the pitching moment coefficient converges to the quasi-steady state in Fig. 8, it shows considerable initial decrease, which corresponds to the initial overshoot for the lift coefficient. Regarding the drag coefficient in Fig. 8, comparison appears also favorable, although the present gives some overprediction in the initial stage.

The aerodynamic response depending on the spoiler deploying rate is presented in Fig. 9. The peak value of adverse lift becomes maximum with the rate 620 deg/s, case C, as observed in the lift curves. The initial decrease of the lift called undershoot is evident for the higher deploying rates; see the curves of cases D, E, and F in Fig. 9. The initial decrease of the pitching moment is observed to become maximum in case C in the pitching moment curves of Fig. 9. Regarding the drag coefficients, the initial overshoot is continuously increased with the deploying rate.

To analyze the aerodynamic mechanism of the adverse lift, the surface pressure coefficients, field distributions of pressure, and instantaneous streamlines are presented simultaneously in Fig. 10 for case D and in Fig. 11 for case E. With rapid deployment of the spoiler, a starting vortex is first formed at the tip of the spoiler. It rapidly grows up to a big bubble, which is extended first to the entire spoiler and then to the trailing edge of the main airfoil. Initially, a strong suction pressure is induced locally by the bubble behind the spoiler: most of its effect is cancelled by the positive pressure buildup upstream of the spoiler and immediately downstream of the bubble as seen with the case $\phi = 45$ deg ($\delta = 13.2$ deg) in Fig. 10. It is attributed to the initial sustaining of the lift as observed in the lift curves of Fig. 9. With increasing spoiler angle the adverse lift presents its maximum value when the vortex bubble is extended just to the trailing edge of the main airfoil; see the case $\phi = 135$ deg in Fig. 10 and the case $\phi = 180$ deg in Fig. 11. This

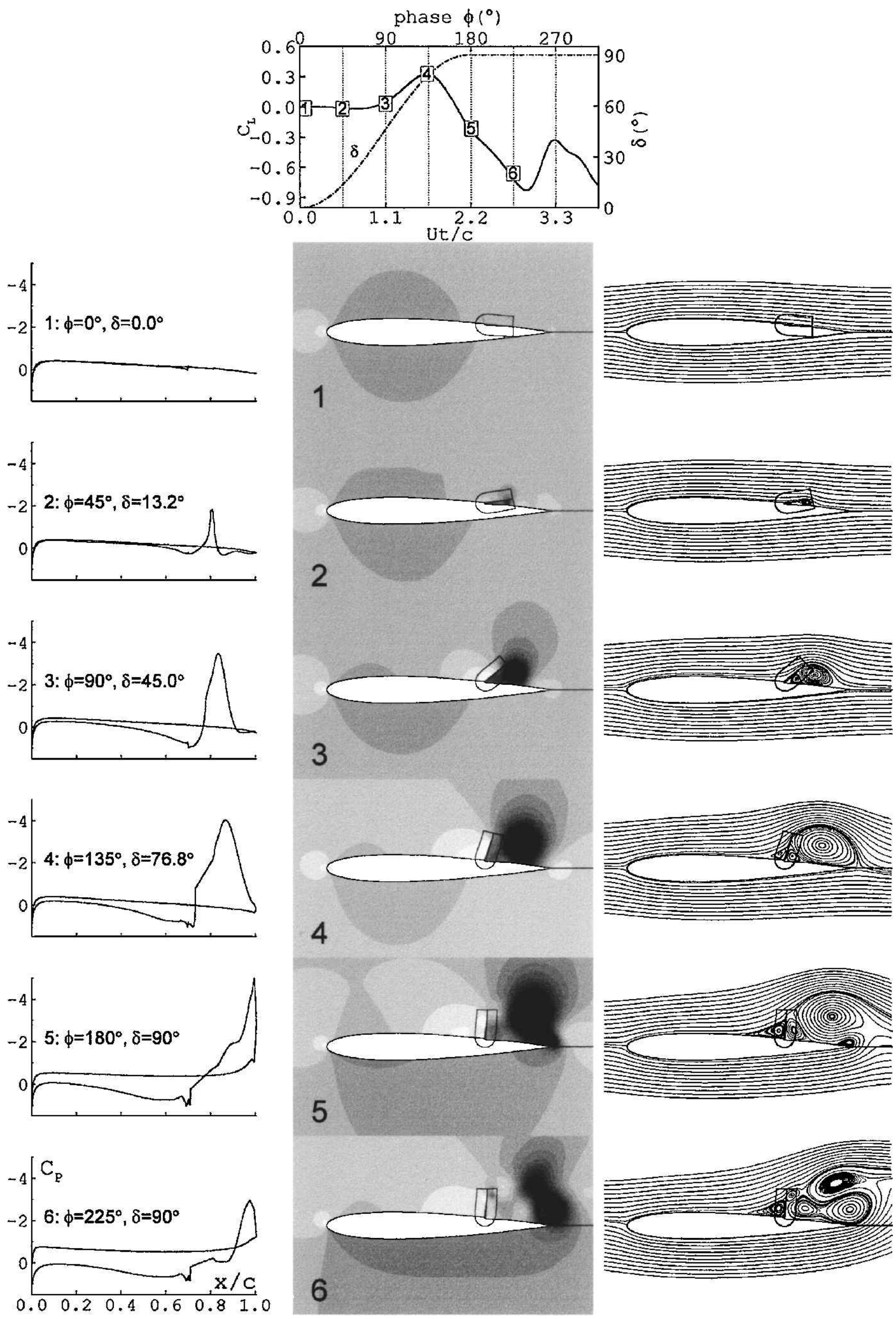

Fig. 10 Flow development by spoiler deployment (case D; ω = 1240 deg/s). Left, Cp curves; middle, pressure distributions; right, instantaneous streamlines.

phenomenon is precisely consistent with Mabey's observation[5] that the reattachment point of the bubble is moved just to the trailing edge in the delay time t_a. After the maximum adverse lift the vortex is burst open as the spoiler is rotated to a larger angle, making the suction pressure decrease in contrast to the positive pressure still building up ahead of the spoiler. A vortex started from the trailing edge of the main airfoil, the rotational direction of which is opposite to the vortex generated by the spoiler, grows rapidly to reduce the size and strength of the spoiler vortex. The separation bubble ahead of the spoiler, the so-called hinge bubbles as referred to in Ref. 7, is generated by the strong adverse pressure gradient upstream of the spoiler erected vertically.

The initial decrease of the lift before it is boosted to an overshoot, an effect not revealed in the earlier experiments and computations, can be explained more by means of the surface pressure coefficient and streamlines in Fig. 11. For the very high deploying rate 2480 deg/s, case D, the spoiler vortex stays near the spoiler despite its high strength; suction pressure appears over a narrow region on the airfoil at the given deflection angle. Further, the strong dynamic effect by the high spoiler deployment rate contributes to increased pressure buildup upstream of the spoiler, spurring undershoot of the lift, which is observed in Fig. 9.

The lift coefficient presented in Fig. 9 is replotted with respect to the phase angle ϕ in Fig. 12. Here, the overshoot (adverse lift), undershoot, and time delay dependent on the deploying rate appear more salient. The maximum value of adverse lift is increasing with the spoiler deploying rate in cases A, B, and C; it decreases in cases D, E, and F. The undershoot is observed in cases D, E, and F, which is increasing with the spoiler deploying rate. The behavior of characteristic time parameters is shown in Fig. 13 with respect to the nondimensional deploying rate. The settling time t_s and time delay t_a of the lift coefficient increase with the deploying rate. The time for the undershoot is first registered at about $\omega c/U = 0.36$ and increases mildly with the deploying rate. The time delay t_a in the present study can be roughly compared with the experimental data from Ref. 11.

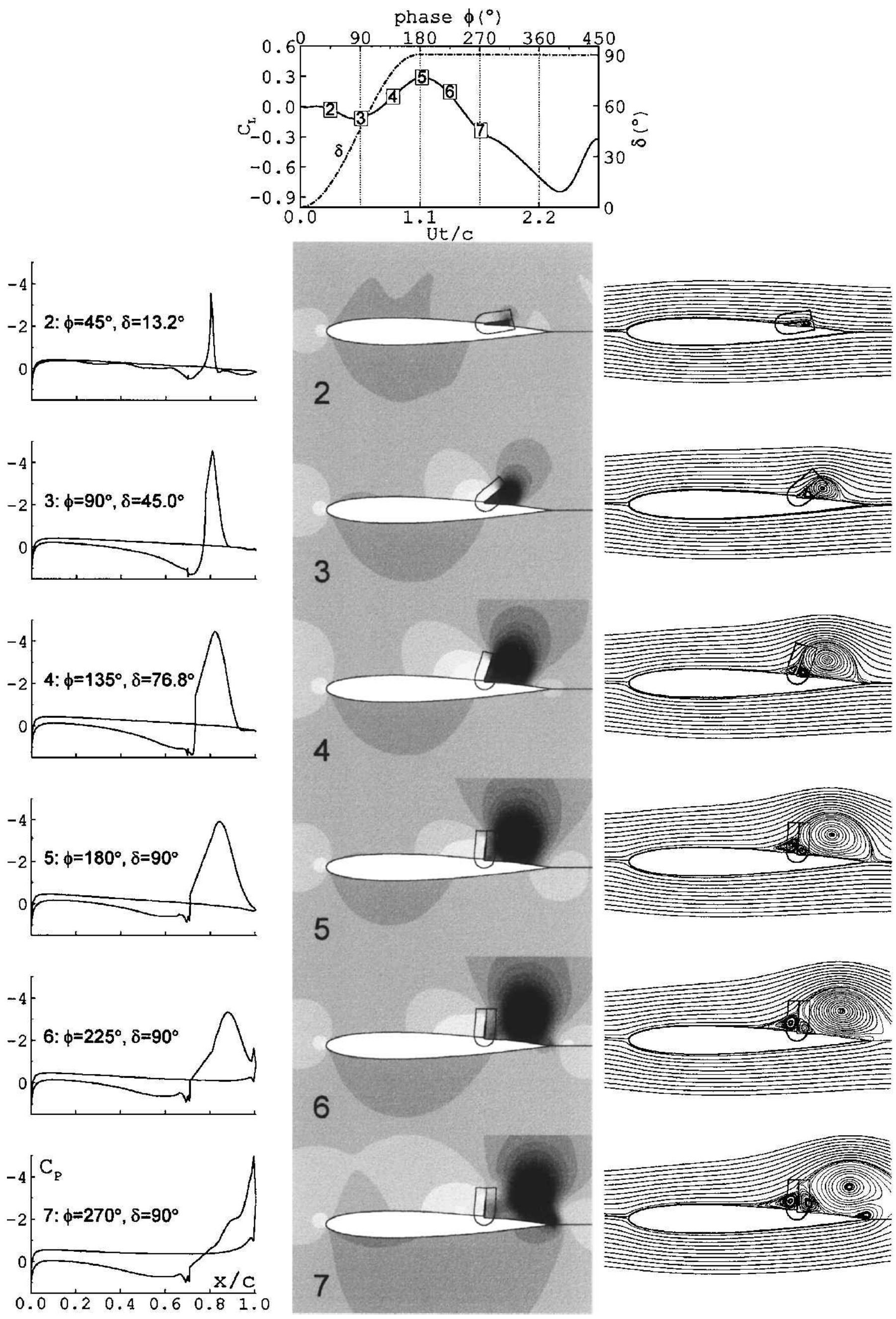

Fig. 11 Flow development by spoiler deployment (case E; ω = 2480 deg/s). Left, Cp curves; middle, pressure distributions; right, instantaneous streamlines.

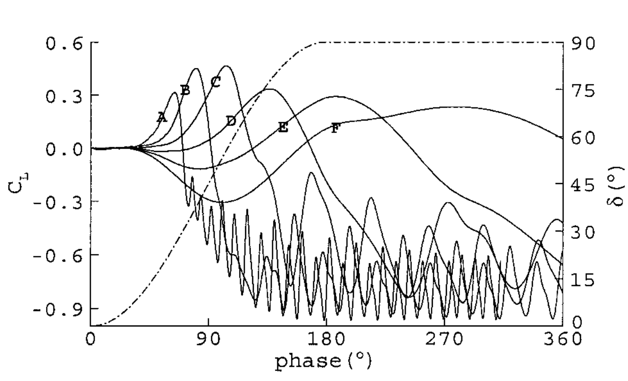

Fig. 12 Response of lift in a phase plane depending on the spoiler deploying rate.

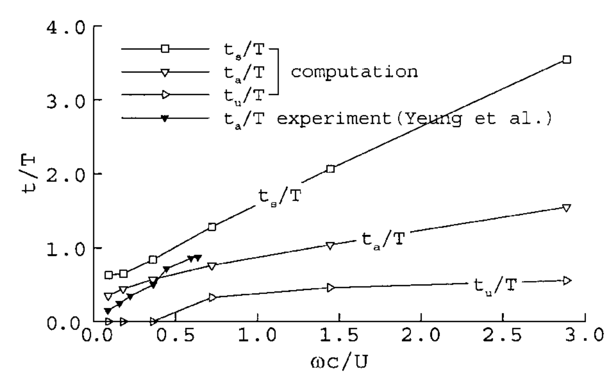

Fig. 13 Characteristic time parameters of the lift coefficient with respect to spoiler deploying rate.

Conclusions

The flowfield around an airfoil with a rapidly deploying spoiler is investigated numerically by solving the turbulent Navier–Stokes equations. The overset grid with the concept of DDDL has awarded a dynamic spoiler grid working very well for a very small hinge gap and very small initial clearance. The time-averaged surface pressure distribution computed for the stationary spoiler has shown good agreement with the experimental data. With a rapidly deploying spoiler the unsteady aerodynamic coefficients showed reasonable agreement with the experimental data. The adverse lift caused by the spoiler vortex is clearly captured and validated; its maximum value is brought in when the reattachment point of the separation bubble just reaches the trailing edge of the airfoil. With increasing spoiler deploying rate the adverse lift is first elevated to a certain degree but decreases afterwards. The initial decrease of lift (or undershoot) is also observed with the higher spoiler deploying rates. Quantitatively more accurate transient aerodynamic data could be expected in the future by some turbulence models tuned to the large-scale separated flows induced by the rapidly deploying spoiler.

Acknowledgment

The authors are grateful to H. Ok for his assistance in developing the present implicit Navier–Stokes code.

References

[1]Mabey, D. G., "A Review of Some Recent Research on Time-Dependent Aerodynamics," *Aeronautical Journal*, No. 1099, Feb. 1984, pp. 23–37.

[2]ESDU International, *ESDU Engineering Science Data*, Controls and Flaps, Vol. 5, No. 90030, 1992, pp. 4–8.

[3]Nelson, R. C., *Flight Stability and Automatic Control*, McGraw–Hill, New York, 1989, pp. 207–210.

[4]Consigny, H., Gravelle, A., and Molinaro, R., "Aerodynamic Characteristics of a Two-Dimensional Moving Spoiler in Subsonic and Transonic Flow," *Journal of Aircraft*, Vol. 21, No. 9, 1984, pp. 687–693.

[5]Mabey, D. G., "On the Prospects for Increasing Dynamic Lift," *Aeronautical Journal*, Vol. 92, No. 1583, 1988, pp. 95–106.

[6]Costes, M., Gravelle, A., and Philippe, J. J., "Investigation of Unsteady Subsonic Spoiler and Flap Aerodynamics," *Journal of Aircraft*, Vol. 24, No. 9, 1987, pp. 629–637.

[7]Lee, C. S., and Bodapati, S., "Experimental Investigation of the Flowfield of an Airfoil with Spoiler," *AIAA Journal*, Vol. 25, No. 11, 1987, pp. 1411–1416.

[8]Nelson, C. F., Koga, D. J., and Eaton, J. K., "Unsteady, Separated Flow Behind an Oscillating, Two-Dimensional Spoiler," *AIAA Journal*, Vol. 28, No. 5, 1990, pp. 845–852.

[9]Tou, H. B., and Hancock, G. J., "Part VI: The Rapid Deployment of a Spoiler on a Two-Dimensional Aerofoil," *Aeronautical Journal*, Vol. 91, No. 910, 1987, pp. 492–498.

[10]Xu, C., and Yeung, W. W. H., "Unsteady Aerodynamic Characteristics of Airfoil with Moving Spoilers," *Journal of Aircraft*, Vol. 36, No. 3, 1999, pp. 530–540.

[11]Yeung, W. W. H., Xu, C., and Gu, W., "Reduction of Transient Adverse Effects of Spoilers," *Journal of Aircraft*, Vol. 34, No. 4, 1997, pp. 479–484.

[12]Ok, H., and Eberhardt, D. S., "Calculation of Flowfield Around an Airfoil with Spoiler," AIAA Paper 93-0527, Jan. 1993.

[13]Kim, J. H., and Rho, O. H., "Numerical Simulation of the Flowfield Around an Airfoil with Stationary or Oscillating Spoiler," *Journal of Aircraft*, Vol. 35, No. 5, 1998, pp. 704–711.

[14]Pulliam, T. H., "Time Accuracy and the Use of Implicit Method," AIAA Paper 93-3360, July 1993.

[15]Ok, H., "Development of the Incompressible Navier–Stokes Solver and Its Application to the Calculation of Separated Flow," Ph.D. Dissertation, Dept. of Aeronautics and Astronautics, Univ. of Washington, Seattle, WA, June 1993.

[16]Venkatakrishnan, V., "On the Accuracy of Limiters and Convergence to Steady State Solutions," AIAA Paper 93-0880, Jan. 1993.

[17]Baldwin, B., and Lomax, H., "Thin Layer Approximation and Algebraic Model for Separated Turbulent Flows," AIAA Paper 78-257, Jan. 1978.

[18]Kim, B. S., "Automatic Multi-Block Grid Generation about Complex Geometries," Ph.D. Dissertation, Dept. of Aeronautics and Astronautics, Univ. of Washington, Seattle, WA, Sept. 1994.